Revue RAMReS – Sciences Appliquées et de l'Ingénieur
RAMReS 2025 - *Published Online 2026*- http://publication.lecames.org/
Vol. 7(1), pp. 47-55, Online January 2026

Vol. 7
ISSN 2630-1164
December 2025

Full Length Research Paper

Multiaxial Fatigue Performance of Flange and Shear Connections in floating offshore wind turbine

Aliou Badara CAMARA[1*], Aboubacar FALL[1], Ndèye Maty NDOYE[1], Séni TAMBA[1], Mamadou Lamine LÔ[1]

[1] Ecole Polytechnique de Thiès, LASTEE, BP : A10 Thiès, Sénégal

Received June 2025 – Accepted October 2025

**Corresponding author. ... abcamara@ept.edu.sn*

Abstract:

This study focuses on the fatigue performance of bolted flange connections and shear bolted connections for offshore wind turbine towers. Offshore wind turbines, which typically consist of a tower supporting the turbine blades, face significant challenges related to the structural integrity of the joints connecting different tower sections. The traditional bolted flange connection is prone to premature degradation due to fatigue loading, limiting its long-term reliability. In contrast, shear bolted connections have shown considerable improvements in fatigue resistance. This paper aims to analyze both connection types, using ANSYS simulations to assess their fatigue behavior based on Dang Van multiaxial fatigue approach. The study demonstrates that shear bolted connections outperform bolted flange connections in terms of durability, with damage in the latter being 2.5 to 4 times greater. The findings provide insights into optimizing tower design and assembly, making them more cost-effective and reliable for offshore wind turbine installations.

Keyword: Offshore wind turbines, Bolted flange connection, Shear connection, Multiaxial fatigue, Damage

Cite this article:
Aliou Badara CAMARA, Aboubacar FALL, Ndèye Maty NDOYE, Séni TAMBA, Mamadou Lamine LÔ (2025). Multiaxial Fatigue Performance of Flange and Shear Connections in floating offshore wind turbine. Revue RAMReS – Sci. Appl. & de l'Ing., Vol. 7(1), pp. 47-55. ISSN 2630-1164.

1. Introduction

Growing concerns about environmental issues have led to an increased adoption of renewable energy sources, including hydropower, solar, and geothermal energy. However, the most significant increase is seen in the exploitation of wind energy. In the past two decades, offshore wind has emerged as a new source of renewable energy. This highlights the requirement for the utilization of larger and more efficient offshore wind turbines (OWTs). The connections used in support structures of OWTs are critical to ensure the excellent structural performance of OWFs[1]. Today, wind energy has become the largest form of power generation capacity in Europe[2]. At sea, the wind potential benefits from higher average wind speeds. This is due to the lower surface roughness at sea[3], which allows for more consistent and less disrupted wind speeds. Floating wind turbines offer a key advantage: their assembly takes place directly at the port, after which they are transported to the site using a conventional tugboat, which can also bring them back to shore for heavy maintenance operations or decommissioning at the end of their life. This feature strengthens the idea that the industry will become economically viable through economies of scale enabled by mass production and the experience gains that will reduce operating costs[4].

Offshore wind turbines (OWT) generally consist of three main elements: the tower, the transition piece (TP), and the foundation. The tower structure is an integral part of wind turbines and includes several bolted connections between the different segments of the tower (Figure 1). This type of configuration is commonly used for most land-based wind turbines with steel towers. What distinguishes offshore wind turbines

is the presence of the TP (in yellow) and the foundation, which connect the base of the tower, located several meters above the maximum water level, to the seabed. The assembly formed by the TP and the foundation is referred to as the substructure of the OWT[5].

However, fixed-foundation wind turbines can only be installed in shallow marine areas, such as those in the southern part of the North Sea, a relatively rare geological configuration. In contrast, the technology of floating offshore wind turbines overcomes this limitation. Supported by several European countries, its development has followed a methodical progression: prototype testing, commissioning of industrial-scale demonstrators, and the current deployment of pre-commercial parks with capacities reaching several tens of megawatts[4].

Figure 1: Illustration of offshore wind turbine tower assemblies

Although there are several types of substructures, the market is currently dominated by monopiles and jackets, representing 81.9% and 6.6% of the installed capacity in 2018[5], respectively. In recent years, however, several offshore wind farms have opted for the bolted circular flange connection, starting with the Amrumbank West offshore wind farm[6]. The Nobelwind wind farm[5][7], commissioned in 2017, was the first offshore wind farm in Belgium to use a bolted connection between the monopile and the transition piece (TP). The Nobelwind farm consists of 50 Vestas 3.3 MW turbines, installed on monopiles (Figure 2a).

However, one of the main factors that will increase the efficiency of current offshore wind turbines is the height of their support towers[8]. This raises several design challenges at the assembly point between the mast and the currently flanged foundation tower, which has a low fatigue resistance. When the swell causes a floating platform to oscillate, it results in cycles of tension and release on the anchoring systems as well as on the elements connecting the platform to the shore, such as pipes or electrical cables[9]. This alternation of stresses accelerates the "fatigue" of materials, causing them to deteriorate much faster than if subjected to a constant load, whether it is permanent tension or compression.

Thus, in order to ensure better performance and improve the competitiveness of the steel tubular tower at higher elevations, it was proposed to replace the existing assembly (flange) with another type, here referred to as a friction assembly. To facilitate the assembly of the tubular sections, elongated holes (Figure 2c) are present on the lower segment. Fasteners can be pre-installed in the standard holes of the upper section and are used to align the angle when it is placed.

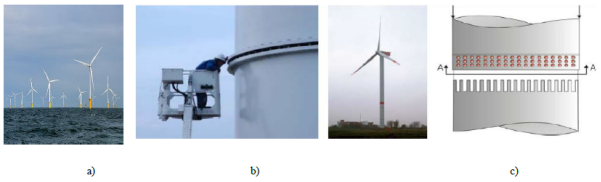

Figure 2: a) Nobelwind[7], b) Existing solution, c) New proposed solution[8],[10]

Thus, the study presented in this article aims to compare the fatigue damage predictions and fatigue life obtained using the multiaxial approach for both the bolted L flange connection and the shear (friction) connection. The first part of the article presents the two types of connections studied. Then the materials properties and the Dang Van multiaxial fatigue are introduced. The finite element model is described, along with the geometric meshing performed using the ANSYS software, the loading cases, and some important details to manage in the context of this study. Finally, the last part compares the results obtained in terms of fatigue damage and fatigue life between the bolted flange connection and the bolted shear connection.

2. Presentation of the bolted assemblies studied

2.1. Bolted L flange connection

Annular flange assemblies with high-strength bolts (Figure 3) are the most common solution for connecting the steel tubular profiles of wind turbine towers. During the design phase, it is essential to prevent the flange connection from opening under service loads. To achieve this, a sufficient preload force

is applied to the bolts. In the event of failure, the flanges separate, which can lead to rupture either in the bolts or in the tower shell.

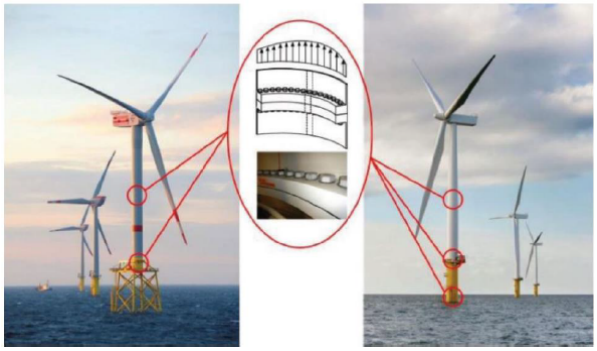

Figure 3: Bolted Flange connection at Offshore Wind Structures[11]

The study of the connection is carried out by considering a T-section (Figure 4). In this approach, a segment of the bolt ring is taken into account, where the tensile stresses acting in the tower shell are incorporated as a concentrated load Z [8, 10, 11].

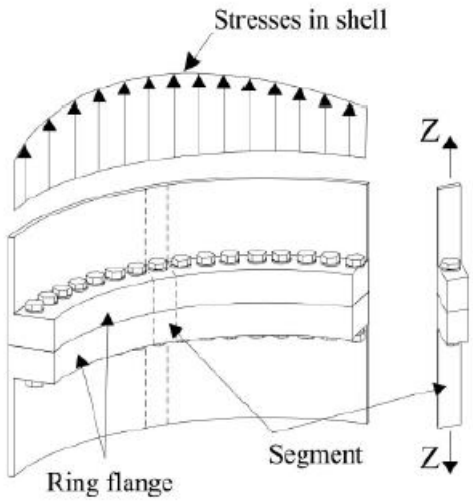

Figure 4: Segment model with internal and external force [11]

The geometry selected for the bolted-L-flange connection is provided in Figure 5.

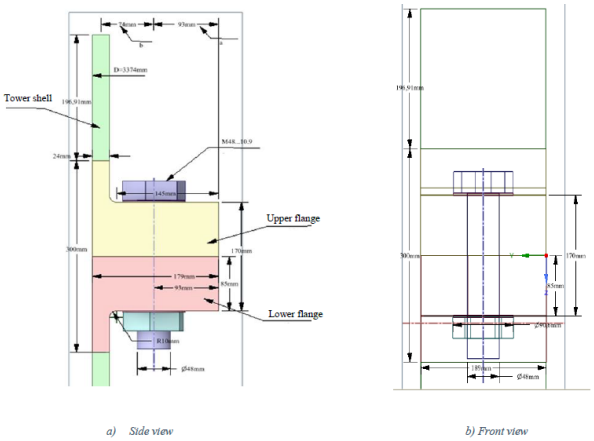

Figure 5: Geometry of the bolted flange connection

The details of the selected geometry is given in table 1.

Table 1: Dimensions of Flanges and Shells

Parameters	a	b	t_f	t_s	c
Values (mm)	93	74	85	24	189

2.2. Bolted shear connection

High strength friction grip connections, or simply friction connections (Figure 6), work by clamping together the plates of the joint by the help of high strength friction grip bolts. These bolts are usually of grade 10.9 or even higher. Load applied on the plates is lead across the connection by friction[8]. Conventional friction connections with standard clearance holes, also known as anti-slip assemblies, have been used in structural engineering for decades. Their behavior has been extensively studied by several researchers and conclusively described by Kulak and al.[12].

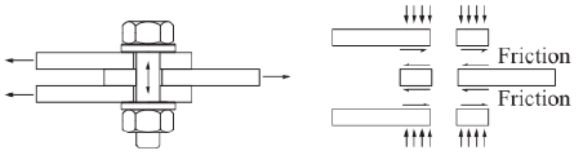

Figure 6: Schematic View of Load Transfer in Friction Connections

The design of friction connections is regulated by the standard EN 1993-1-8[13], which distinguishes between slip resistance at the serviceability limit state (Category B) and at the ultimate limit state (Category A). The calculation of slip resistance mainly depends on the friction properties of the connected surfaces and the preload in the engaged bolts[13].

$$F_{S,Rd} = \frac{k_s \times n \times \mu}{\gamma_{M3}} \times F_{p,c} \qquad \text{[Eq. 1]}$$

Where

k_s is a factor that takes into account the shape and size of the hole

n is the number of interfaces in contact

μ is the coefficient of friction

$F_{p,c}$ is the preload of the bolt.

The geometry selected for the bolted shear connection is given in Figure 7.

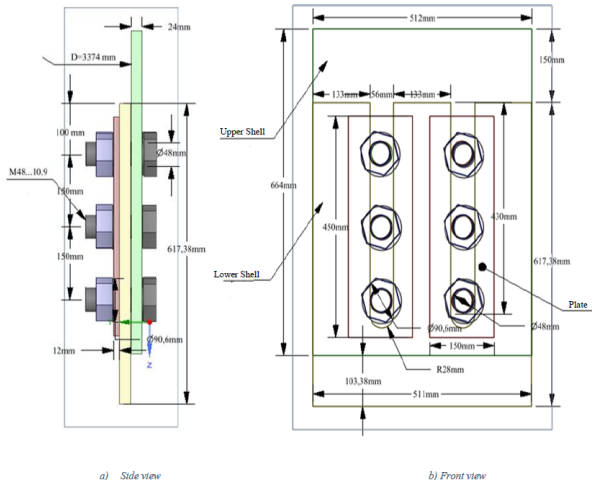

Figure 7: Geometry of the bolted shear connection

2.3. Material mechanical properties

The steel used for both connections has a Young's modulus of 210 GPa and a Poisson's ratio of 0.3. The mechanical properties of the flanges and the shells are provided in table 2.

Table 2: Mechanical properties of Flanges and Shells

Stresses (MPa)	Flange	Shell
f_y	300	355
f_u	480	470

The mechanical properties of the bolts used are given in table 3.

Table 3: Mechanical properties of M48 Bolts -10.9 Class

Bolt M48 – 10.9		
Parameters	Values	Units
d	48	mm
d_0	50	mm
f_{ub}	1000	MPa
f_y	900	MPa
A_S	1473	mm²

Failure of both types of connections often occurs at stress levels lower than the ultimate force. The variable nature of the loads on wind turbines makes them vulnerable to fatigue.

3. Material fatigue

It is essential to integrate fatigue analysis from the design stage to ensure the reliability of components. Traditionally, a prototype is created and tested for endurance, but this approach is costly and slow[14]. Nowadays, the goal is to reduce in-service testing by using software tools that allow for rapid simulation of a component's fatigue behavior under random multiaxial loads. These tools not only predict the fatigue response but also optimize the design by adjusting safety margins. As a result, the design is optimized for fatigue resistance even before the prototype is built, thus reducing costs and development time. The most complex type of loading a material can undergo is variable amplitude multiaxial loading, often referred to as "random multiaxial," although this is not necessarily associated with a statistical nature. In high-cycle fatigue, multiaxial criteria are used to account for the multiaxial component of the stresses experienced by the material. This article presents an analysis of constant amplitude multiaxial fatigue for the two bolted assemblies, using the Dang Van criterion.

3.1. Dang Van multiaxial fatigue criterion

The Dang Van criterion in its version of 1973 is the first multiaxial fatigue criterion that was introduced in the French industry. It was originally presented through considerations established at the microscopic scale, even if the criterion uses macroscopic stresses which are the alternating part of the shear stress τ_{ha} and the hydrostatic pressure p[15],[16]. The fatigue damage function E of the criterion gives a maximization of the damage indicator E_h, defined on the material plane which unit normal vector is h:

$$E_h = \max_t \left\{ \frac{\tau_{ha}(t) + \alpha.p(t)}{\theta} \right\} \quad \text{[Eq. 2]}$$

Where

p(t) is the hydrostatic pressure,

$$p(t) = \frac{I_1(t)}{3} = \frac{\sigma_{11}(t) + \sigma_{22}(t) + \sigma_{33}(t)}{3}$$

$I_1(t)$ is the time dependent first invariant of the stress tensor,

$\tau_{ha}(t)$ is the alternating shear stress acting at time t on the material plane; it is obtained by determining the smallest circle surrounding to the load trajectory as defined by Kenmeugne et al.[17].

The plane where E_h is maximal is the so-called critical plane. It allows the criterion to express the material fatigue damaging affect generated by the multiaxial loading cycle. The fatigue function of the criterion is thus written as:

$$E_{DV} = \max_h (E_h) \quad \text{[Eq. 3]}$$

The fatigue function of the criterion is equal to unity when the fatigue limit of the material is reached by the analyzed multiaxial stress cycle. This fatigue function (E_{DV} =1) is also checked for particular material fatigue limits as those related to fully reversed tension fatigue limit (σ_{-1}, R = -1), fully reversed torsion fatigue limit (τ_{-1}, R = -1). This allows to calibrate the criterion, i.e to determine the two parameters α and θ that are involved within the damage indicator formulation.

$$\begin{cases} \alpha = 3\left(\frac{\tau_{-1}}{\sigma_{-1}} - \frac{1}{2}\right) \\ \theta = \tau_{-1} \end{cases} \quad \text{[Eq. 4]}$$

3.2. S-N curves

The S-N curves (stress-life curves) are essential for understanding the fatigue behavior of materials. They illustrate the relationship between the applied stress amplitude on a material and the number of cycles it can withstand before failure. Various S-N curve models exist in the literature, including Wohler's model, Basquin's model, Stromeyer's model, and Bastenaire's model, among others [18]. The model used in this study is derived from the DNV-RP-C203 standard[19]. It is applicable to high-strength steels with a yield strength greater than 500 MPa, which is the case for the M48-10.9 bolts used in this analysis.

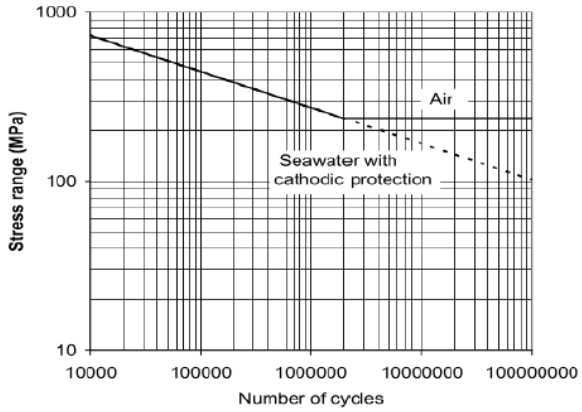

Figure 8: S-N curve for high strength steel [19]

$$\text{Log}\,N = 17.446 - 4.70\log[2\sigma_{-1}(N)]$$

$$\sigma_{-1}(N) = 10^{3.41-0.21\text{Log}(N)} \qquad \text{[Eq. 5]}$$

Where N is the number of cycles and σ_{-1}, the alternating part of the stress

The calibration of Dang Van criterion requires knowledge of two S-N curves. Hence the S-N curve for fully reversed alternating tension σ_{-1} (N) and the S-N curve for fully reversed alternating torsion τ_{-1} (N) are used for this purpose. These fatigue limits are used for the determination of the parameters α and θ (Eq 4). The S-N curve for fully reversed alternating torsion τ_{-1} (N) is derived from σ_{-1} (N) using the equation 6.

$$\frac{\sigma_{-1}(N)}{\tau_{-1}(N)} = \frac{\sigma_e}{\tau_e} = \sqrt{3} \qquad \text{[Eq. 6]}$$

Indeed, according to Zenner and Simbürger[20] , the ratio between σ_{-1} (N) and τ_{-1} (N) can vary between 1.25 and 2 for ductile materials.

3.3. Flowchart of the multiaxial fatigue post-treatment tool

Multiaxial stress states are observed on the studied bolted connections especially in stress concentration zones. A multiaxial fatigue post-treatment tool is thus implemented on Matlab software using the Dang Van multiaxial fatigue criterion (critical plane approach). The fatigue post treatment tool developed and validated by Camara [18] is use to analyse bolts behaviour from the fatigue point of view. The flowchart of the iterative process is given in figure 9.

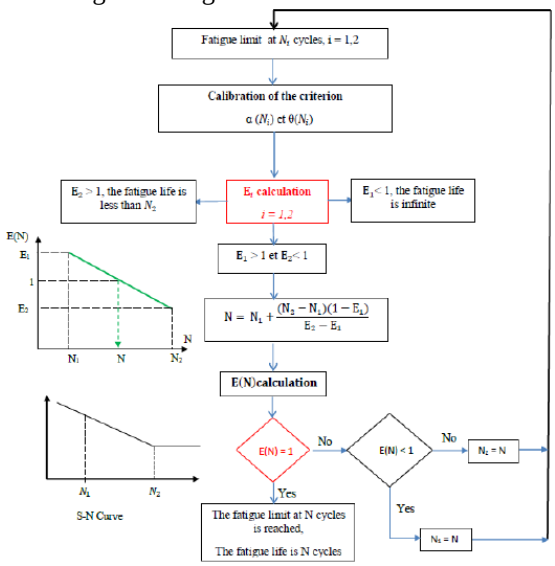

Figure 9: Flowchart of the iterative procedure for assessing fatigue life with Dang Van criterion

Convergence of the approach is progressive and proceeds by reducing the domain [N_1, N_2] of the solution sought at each iteration:

- If E(N) > 1, N_1 takes the value of N that of N_2 is unchaged;
- If E(N) < 1, N_2 takes the value of N that of N_1 is unchaged.

The value of N corresponding to E(N) = 1 by linear interpolation of the two points
(N_1, E_1) et (N_2, E_2) is given by equation 7.

$$N = N_1 + \frac{(N_2 - N_1)(1 - E_1)}{E_2 - E_1} \qquad \text{[Eq. 7]}$$

The process is stopped when the absolute difference between E(N) and the unit value is deemed sufficiently small (e.g. 10^{-4}). Convergence is very rapid, since only the criterion's calibration constants α(N) and θ (N) are modified from one iteration to the next, while all the stress components of the cycle analyzed remain identical. Extended in this way to the field of limited endurance, multiaxial fatigue criteria are transformed into tools for determining multiaxial fatigue life. This multiaxial fatigue post treatment tool was validated in[18].

When a structure in service is subjected to periodic multiaxial loading, it is highly likely that this loading will cause damage or even failure of the structure, even if it is below the material's yield limit, provided it is applied a sufficient number of times. To quantify this fatigue damage in multiaxial loading, we use fatigue criteria.

When applied to a multiaxial stress cycle, a fatigue criterion allows us to position any stress cycle relative to the material's endurance limit (or relative to its fatigue limit at N cycles). It expresses, through the value of its fatigue function E, the more or less damaging nature of the applied stress cycle.

The multiaxial fatigue post-treatment tool developed on Matlab software and validated by Camara [18] is used to assess the fatigue damage and then the fatigue life of the bolt in both connections.

4. Results and Discussion

4.1. Finite Element Model

The study of the multiaxial fatigue behavior of the bolted flange connection and the bolted shear connection requires a thorough understanding of the stress states on both the assembled components and the connecting elements, specifically the M48.10.9 bolts. To better understand how stresses are distributed within the assembly between the tower and the foundations of a floating offshore structure, a finite element analysis is performed. This process involves modeling the assembly, composed of several components and links, into a series of finite elements (nodes). These elements form a complex mesh, allowing a detailed representation of the behavior of the entire system under various loads. This simulation enabled us to determine the stresses applied to each node of the connection. These stress states are essential for the multiaxial fatigue analysis to determine the damage and fatigue life of the bolts in each connection. The geometries of both connections are given in figures 5 and 7.

4.1.1. Contact management and meshing

Contact management is a crucial step in this study. Considering contact introduces an additional non-linearity in the finite element modeling. Contact-type nonlinearities are among the most challenging to handle because they involve abrupt changes in behavior (during contact-separation transitions and adhesion-sliding transitions[18].

For the bolted flange connection (figure 5), a fully bonded contact is used, except at the contact between the two flanges, where a frictionless contact is applied Bonded contact means no penetration, no separation, and no sliding is accepted.

Regarding the bolted shear connection in figure 7, a frictional contact is applied at the interface between the upper shell and the lower shell on one side, and on the other side, the contact between the shell and the plate.

The meshes shown in figure 10 are used for element analysis. The bolt, consisting of the screw, nut, and washers, is finely meshed with a mesh size of 10 mm. The two flanges (upper and lower flanges) in figure 10a have a mesh size of 20 mm, while the shell part has a mesh size of 30 mm. The plate and shells of the bolted shear connection (figure 10b) are meshed with elements of 20 mm in size.

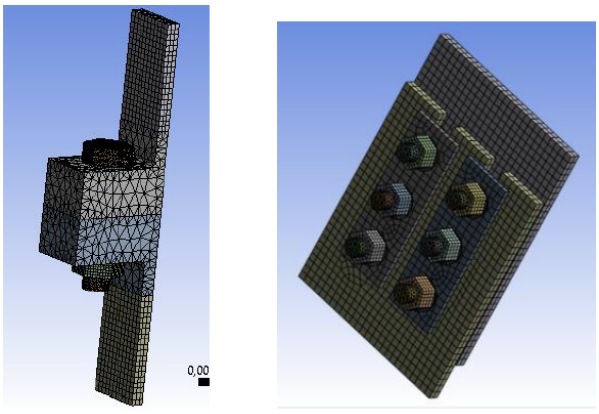

Figure 10: a) Bolted flange connection meshing, b) Bolted shear connection meshing

4.1.2. Contact management and meshing

Three loading cases are analyzed for each connection to better understand their impact on the fatigue resistance of the bolts in both types of connections. Table 4 presents the three studied loading cases. The loading configurations for the six-bolt in the shear connection are derived from the single-bolt configuration of the flange assembly by multiplying the load by six. The preload for each bolt is 150 kN, as illustrated in Figure 11.

Table 4: Loading cases

Cases	Loading (kN)		Preload (kN)
	Flange connection	Shear connection	
Case 1	84	500	150
Case 2	8.4	50	
Case 3	3.4	20	

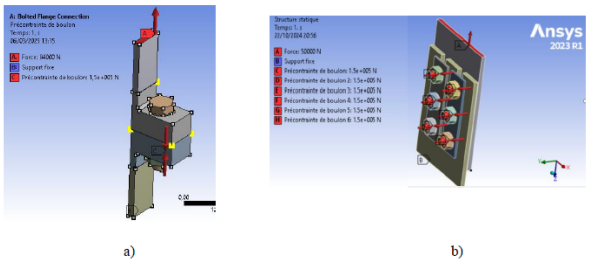

Figure 11: a) Loading case 1 of the bolted flange connection; b) Loading case 1 of the bolted shear connection

The external loading is applied cyclically to describe the loading history, enabling a constant amplitude fatigue analysis. Figure 12 illustrates the loading cycle applied to the flange assembly in case 1.

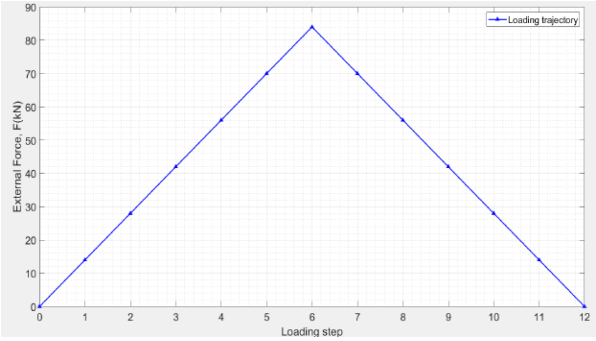

Figure 12: Illustration of the load cycle on the bolted flange connection in case 1

Repeated tensile loading on the bolted flange connection leads to the opening of its two parts, thereby generating a complex stress state involving both tension and bending at the bolt (figure 13a). In contrast, in the bolted shear connection, the bolts are subjected solely to shear stresses (13b). Therefore, to accurately assess performance in terms of damage and durability, the multiaxial fatigue behavior of the bolts in both connections must be analyzed under identical loading conditions. This approach will provide a deeper understanding of the fatigue resistance of these two types of connections.

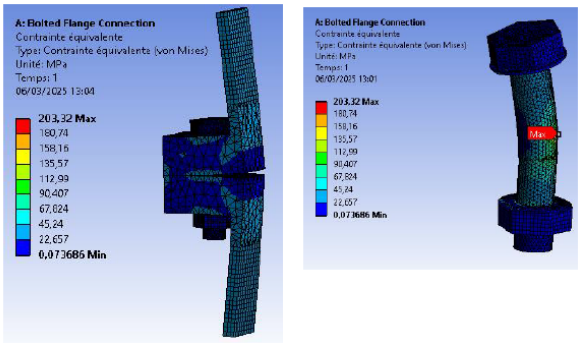

a) Loading Case 1 of the bolted flange connection

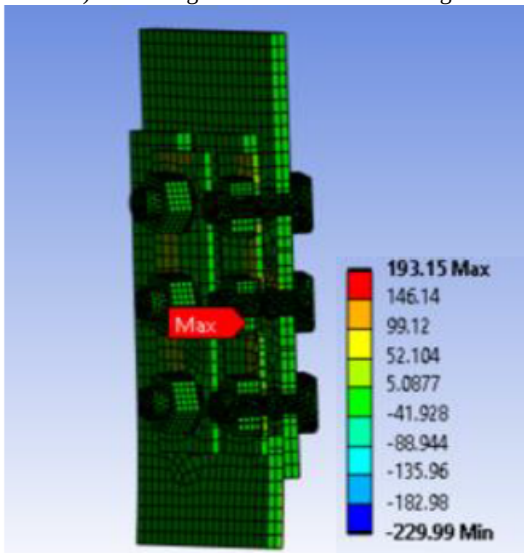

b) Loading Case 1 of bolted Shear connection

Figure 13: Von Mises stress distribution up on the bolted flange connection and the bolted Shear connection

4.2. Multiaxial fatigue damage and fatigue life assessment

The fatigue damage is assess at the endurance limit (2.10^6 cycles). The analysis of the multiaxial fatigue performance of the two types of connections shows the same trend in terms of damage at the endurance limit (figures 14) as well as in terms of fatigue life expressed in number of cycles (figure 15).

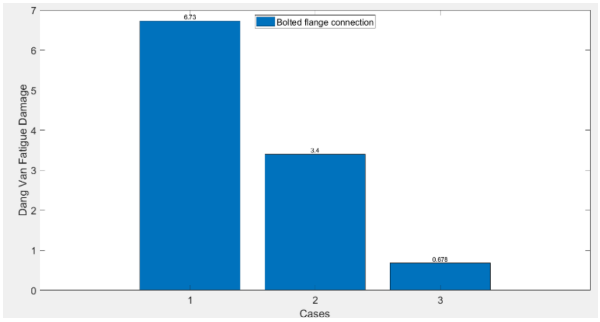

a) Bolted flange connection results

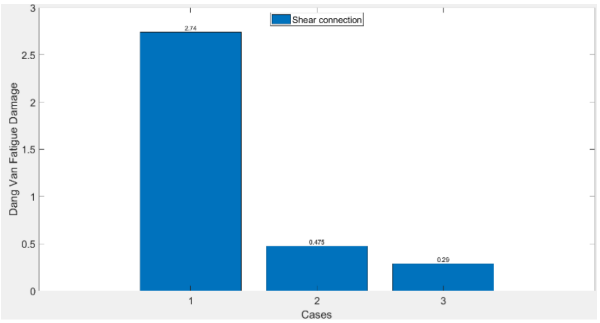

b) Bolted shear connection results

Figure 14: Dang Van fatigue damage

As the external load decreases, we observe a reduction in the damage indicator in both the flange connection and the shear one. Additionally, greater damage is observed in the bolted flange connection compared to the bolted shear connection (figure 14). This indicates that the bolt is more stressed in the flange connection (Figure 13), leading to premature fatigue failure in this configuration. Indeed, the bending moment caused by the eccentricity of the external force relative to the bolt axis can explain the significant damage in the bolted flange connection, especially since the moment is absent in the bolts of the shear assembly.

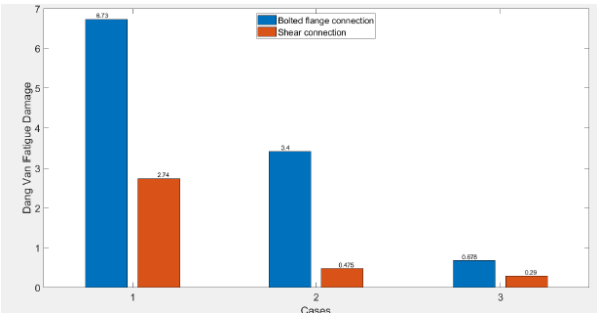

Figure 15: Dang Van fatigue damage comparison

Damage is inversely proportional to fatigue life, meaning that a decrease in damage directly leads to an increase in fatigue life, and vice versa. Thus, an analysis of the fatigue life of the bolt in the two connections shows a significant increase in multiaxial fatigue life as the external load decreases. The predicted fatigue life is higher for the bolted shear connection (figure 16).

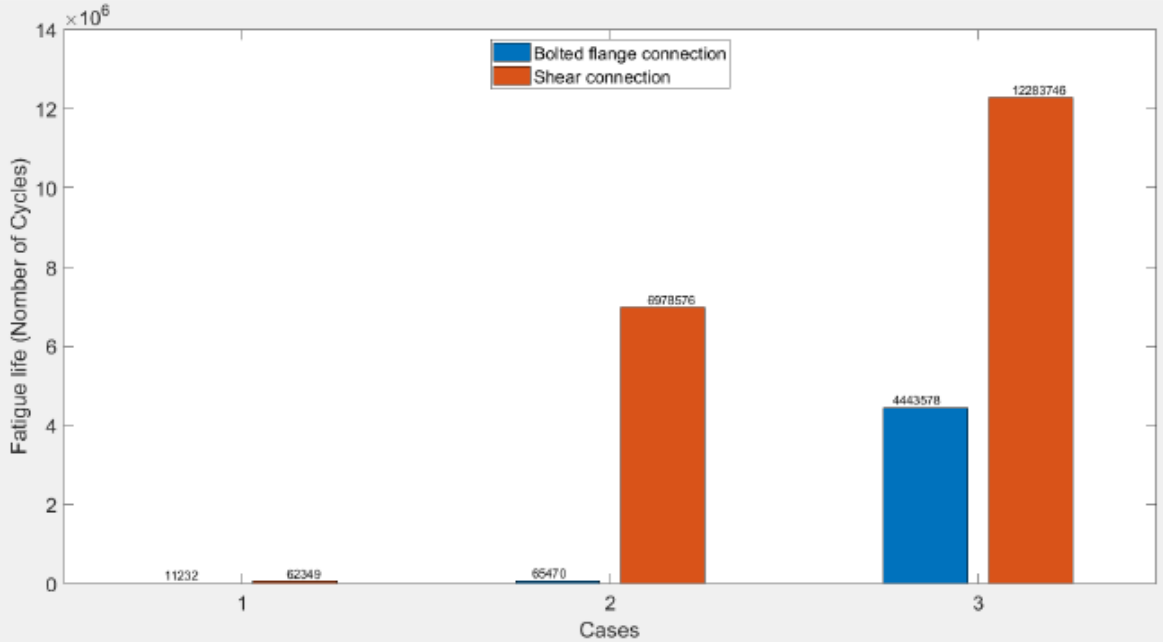

Figure 16: Multiaxiale fatigue life with Dang Van Criterion

The shear connection therefore offers better fatigue performance for this analysis, ensuring durability under variable and demanding loading conditions. The bolted flange connection, although effective under more moderate loads, remains limited due to the complexity of the stresses it experiences.

4. Conclusion

In light of this analysis of bolt performance in the assembly between the tower and foundations for floating offshore structures, where external loads, stress triaxiality, and fatigue play a critical role in the component's fatigue life, the bolted shear connection offers better resistance to multiaxial fatigue. Its simplicity in terms of load distribution on the bolts (mainly in shear) minimizes critical stress concentrations and reduces the risk of premature cracking. The bolted flange connection, while effective for moderate loads, is more sensitive to multiaxial fatigue due to the complexity of the stresses present (bending, tension, shear). Even with high preload, damage remains significant, leading to shorter fatigue life under high loads. Ultimately, the choice of assembly type should be guided by the specific requirements of the project. For structures requiring high tolerance to fatigue under variable and complex loads, the bolted shear connection provides a more robust solution.

REFERENCES

[1] L.CHENG. Assessment of bolted connections for supporting structures of offshore wind turbine towers - Mechanical performance and structural health monitoring, Delft University of Technology, 2023. https://doi.org/10.4233/uuid:fb1e3e10-0495-43e8-a53c-299062dbe58f

[2] R. Ryndzionek and Ł. Sienkiewicz. Evolution of the HVDC link connecting offshore wind farms to onshore power systems, Energies, vol. 13, no. 8, 2020. https://doi.org/10.3390/en13081914

[3] I. Troen, L. Petersen. European wind atlas, Risø National Laboratory,1989. https://orbit.dtu.dk/en/publications/european-wind-atlas

[4] M. Cruciani. L'éolien offshore flottant dans sa dimension industrielle et technologique, IFRI Centre Energie, 2019.

[5] W. Weijtjens, A. Stang, C. Devriendt, P. Schaumann. Bolted ring flanges in offshore-wind support structures, Journal of Constructional Steel Research, 2021. https://doi.org/10.1016/j.jcsr.2020.106361

[6] RWE AG, Amrumbank West offshore wind farm, 2020. https://www.rwe.com/en/the-group/countries-and-locations/amrumbank-west-offshore-wind-farm/

[7] Nobelwind, Offshore wind energy power plant – Annual work report 2021, 2022.

[8] C. Heistermann. Behaviour of Pretensioned Bolts in Friction Connections, Licentiate thesis, 2011)

[9] G. Bracq, l'éolien offshore flottant

[10] C. Heistermann. Resistance of Friction Connections with Open Slotted Holes in Towers for Wind Turbines, Doctoral Thesis, 2014.
[11] R. K. Altes. Influence of geometric imperfections and increasing turbine sizes on validity load transfer functions in bolted ring-flange connections, Delft University of Technology, 2023.
[12] G. L. Kulak, J. W. Fisher, and J. H. A. Struik. Guide to Design Criteria for Bolted and Riveted Joints,American Institute of Steel Construction, 2001.
[13] EN 1993-1-8 - Eurocode 3: Design of steel structures - Part 1-8: Design of joints, vol. 33, pp. 1-135, 2005.
[14] B. Weber. Fatigue multiaxiale des structures industrielles sous chargement quelconque, Thèse,INSA Lyon, 1999.
[15] K. Dang Van, O. Griveau, B Message. On a new Multiaxial Fatigue Limite Criterion : Theory and Application, Proceedings of the International Conference on Biaxial/Multiaxial Fatigue, University of Sheffield, pp. 479-496, 1989.
[16] K. Dang Van, A. Le Douaron, H. P. Lieurade. Multiaxial fatigue limit: a new approach, Proceedings of the 6th International Conference on Fracture (ICF6), New Delhi, India, 4–10 December 1984, pp. 1879-1885, 1984.
[17] B. Weber, B. Kenmeugne, J.C. Clement, J. L. Robert. Improvements of multiaxial fatigue criteria computation for a strong reduction of calculation duration, Comput. Mater. Sci., vol. 15, pp. 381-399, 1999.
[18] A. B. Camara. Analyse du comportement en fatigue d'assemblages boulonnés. Thèse, Université Clermont-Auvergne, pp. 1-201, 2019.
[19] Recommended Practice DNVGL-RP-C203 : Fatigue design of offshore steel structures, pp. 1-18, 2005.
[20] J. L. Harald Zenner, Armin Smbürger. on the fatigue limit of ductile metals under complex multiaxial loading, Int.J. of fatigue, pp. 137–145, 2000.